JCTC Journal of Chemical Theory and Computation

pubs.acs.org/JCTC Addition/Correction

Correction to "Excited-State Absorption: Reference Oscillator Strengths, Wave Function, and TDDFT Benchmarks"

Jakub Šiňůček, Boris Le Guennic,* Yann Damour, Pierre-François Loos,* and Denis Jacquemin*

J. Chem. Theory Comput. **2025**, *21* (9) 4688−4703. DOI: 10.1021/acs.jctc.5c00159

Cite This: https://doi.org/10.1021/acs.jctc.6c00505 Read Online

ACCESS | Metrics & More | Article Recommendations | Supporting Information

There were some inconsistencies concerning the ESA oscillator strengths of carbon monoxide in the original work.

First, for the doubly degenerate $\Pi \rightarrow \Pi$ transition, the published values are correct for all methods. However, unlike in the case of the doubly degenerate benzene transition, they should be multiplied by 2 instead of 4 for carbon monoxide to allow comparisons with experiment, since among the four possible combinations, only two have significant *f*. Hence, the statement made on p. 4692 just before Section 3.1 is not fully correct.

Second, for all TD(A)-DFT calculations, the three singly degenerate transitions of carbon monoxide, i.e., $2\Sigma^+ \rightarrow 2\Pi$, $1\Pi \rightarrow 2\Sigma^+$, and $1\Pi \rightarrow 3\Sigma^+$ were treated incorrectly. The originally published values were incorrectly multiplied by 2 for TD(A)-DFT results during the statistical analysis.

Therefore, while the wave function statistics of the original paper, as well as the energy statistics for all methods, are correct, the TD(A)-DFT statistics are slightly altered (see below). We provide new Supporting Information with corrected data, as well as the corrected Figures 5−8 and 10 below.

The key changes are

1. TD-CAM-B3LYP is even more accurate than originally reported and becomes very competitive with respect to QR-CC2 and, in some cases, even QR-CCSD.
2. The overall trends among the tested functionals remain the same, with BH&HLYP swapping place with LC-BLYP47 by a small margin.
3. The errors of all functionals for small molecules (1−3 non-hydrogen atoms) become smaller. The general trends and qualitative conclusions regarding the impact of the system size are, however, unaffected.
4. The largest changes are logically obtained for the small subset of transitions used for the estimate of the geometry relaxation (Section 3.4). The error metrics of all TD(A)-DFT determined on the optimal S_0 drops significantly, and they all become very competitive with QR-CC2 and even QR-CCSD. Their order changes as well, with CAM-B3LYP moving, gratifyingly, to the top spot in terms of MAE.
5. In contrast, the statistical indicators for the same subset but using the excited-state geometries do not change significantly, and the original functional order is conserved. This means that the deterioration of *f* accuracy when moving from optimal ground geometries to their excited-state counterparts increases.

As a consequence of the above, the two last sentences of the paragraph preceding Section 3.1 should read:

> In the case of ESA, if both states involved in the transition are degenerate, one has to multiply the corresponding value of *f* by four for, e.g., the $E_{1g} \rightarrow E_{2u}$ transition and two for, e.g., the $\Pi \rightarrow \Pi$ transition. In this work, we publish *f* of only one of the degenerate states/transitions, and we highlight the degenerate states with an asterisk (*).

The last sentence of p. 4696 should read:

> For full TD-DFT, the ranking is as follows: CAM-B3LYP (0.011), LC-BLYP33 (0.024), BH&HLYP (0.026), LC-BLYP47 (0.028), and B3LYP(0.034).

The last sentence of the second paragraph of p. 4697 should read:

> Quite interestingly, CAM-B3LYP even outperforms both QR-CC2 and ISR-ADC(2) in terms of MAE, RMSE, and SDE.

The last paragraph of Section 3.4 (pp. 4699−4700) should read:

> Let us now look at the ESA f values in the length gauge (Figure 10). Going from S_0 to $S_{1/2}$ structures induces only a negligible deterioration of the performance of wave function methods, with the exception of ISR-ADC(2), but a significant drop in performance for TD(A)-TDDFT. The difference between the $S_{1/2}$ and S_0 *f* MAE of wave function methods grows in the following series: ISR-ADC(3) (0.000), QR-CCSD (0.002), EOM-CCSD (0.003), QR-CC2 (0.003), ISR-ADC(2) (0.008). The general trends are therefore unaffected by the selected geometry. For full TD-DFT, the increase of MAE (RMSE) at the $S_{1/2}$ geometry is LC-BLYP33: 0.016 (0.063), CAM-B3LYP: 0.018 (0.059), LC-BLYP47: 0.019 (0.061), BH&HLYP: 0.022 (0.075), B3LYP:

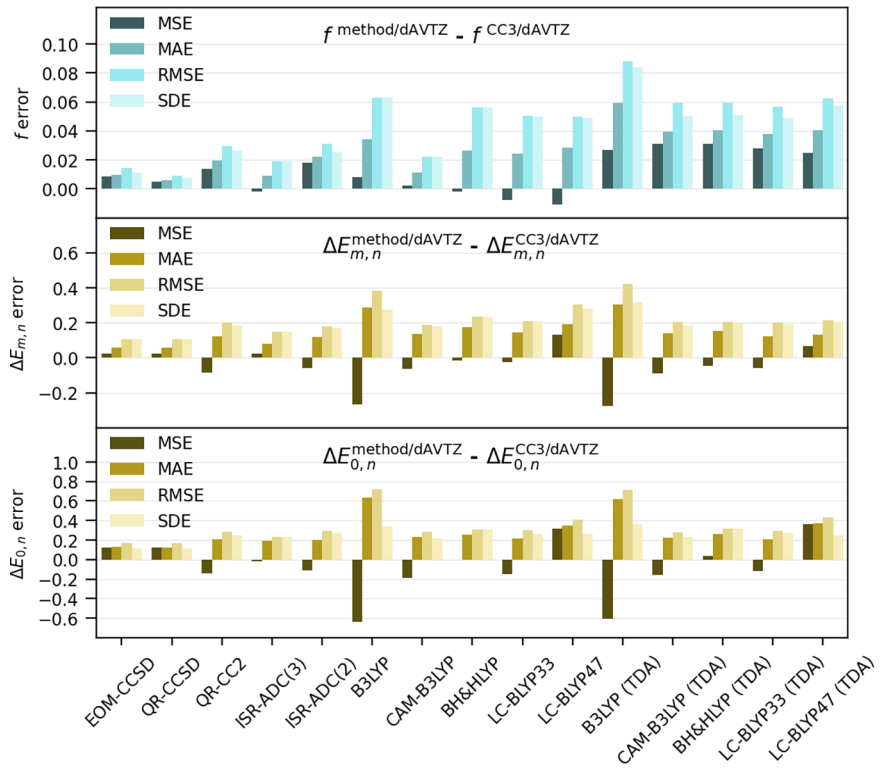

Figure 5. Comparison of MSE, MAE, RMSE, and SDE for all methods. Top: f, in length gauge. Center: $\Delta E_{m,n}$ in eV. Bottom: $\Delta E_{0,n}$ in eV. $\Delta E_{m,n}$ and f values are compared with QR-CC3/dAVTZ and $\Delta E_{0,n}$ with CC3/dAVTZ.

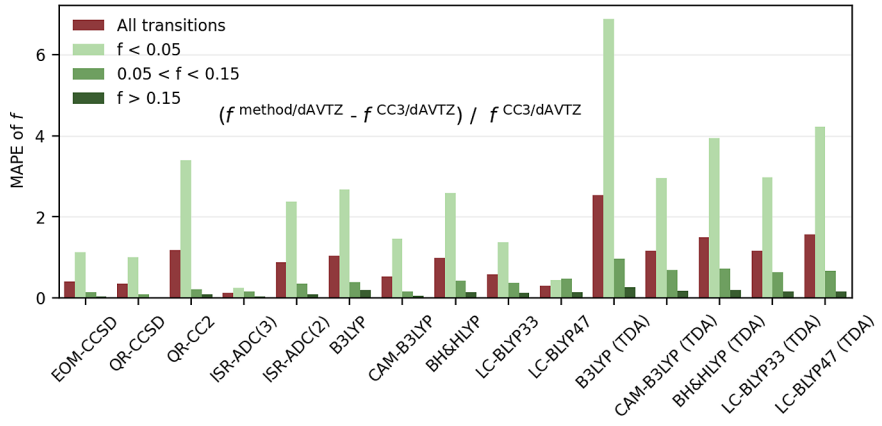

Figure 6. Comparison of MAPE in f values of all methods divided by the magnitude of the computed f into three groups: $f < 0.05$, $0.05 < f < 0.15$, and $f > 0.15$. The reference values are obtained at the CC3/dAVTZ level in the length gauge.

0.023 (0.069), whereas for TDA, one gets: LC-BLYP47: 0.007 (0.016), B3LYP: 0.015 (0.033), LC-BLYP33: 0.018 (0.046), BH&HLYP: 0.020 (0.045), CAM-B3LYP: 0.022 (0.047). Given this nonuniform behavior of XCFs, the ranking of functionals based on MAE (full TD-DFT), on this subset of transitions, changes from CAM-B3LYP (MAE = 0.006), BH&HLYP (MAE = 0.008), LC-BLYP33 (MAE = 0.009), B3LYP(MAE = 0.011), and LC-BLYP47 (MAE = 0.011), on S_0 geometry, to CAM-B3LYP (MAE = 0.024), LC-BLYP33 (MAE = 0.025), LC-BLYP47 (MAE = 0.030), BH&HLYP (MAE = 0.030), and B3LYP(MAE = 0.034) on $S_{1/2}$ geometry. Therefore, from this limited subset, it appears that CAM-B3LYP remains a functional of choice. In short, all XCFs seem to yield larger errors when going away from the Franck−Condon region, though it is unclear if the trends in performance are significantly altered or not.

■ ASSOCIATED CONTENT

Supporting Information

The Supporting Information is available free of charge at https://pubs.acs.org/doi/10.1021/acs.jctc.6c00505.

Geometries for all compounds. Additional results for all methods and basis sets (PDF)

https://doi.org/10.1021/acs.jctc.6c00505
J. Chem. Theory Comput. XXXX, XXX, XXX−XXX

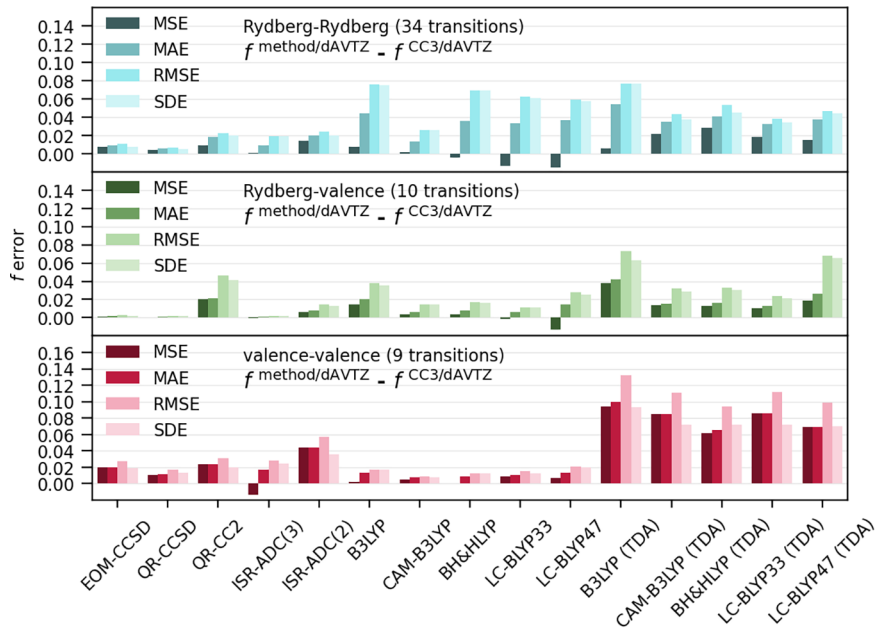

Figure 7. Comparison of errors in *f* for all methods divided by the character of the states involved. Top: Rydberg−Rydberg. Center: Rydberg−valence. Bottom: valence−valence. See the caption of Figure 5 for more details.

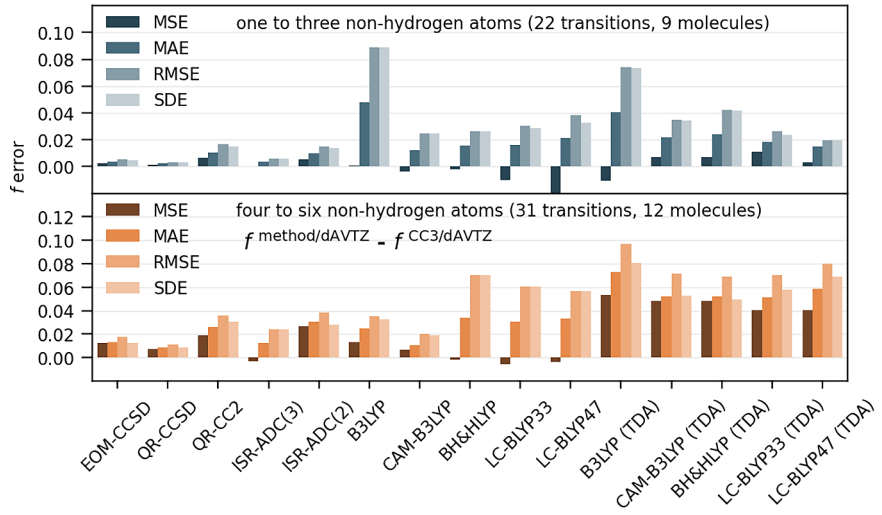

Figure 8. Comparison of errors in *f* for all methods depending on the molecular size. Top: 1−3 non-hydrogen atoms. Bottom: 4−6 non-hydrogen atoms. See the caption of Figure 5 for more details.

https://doi.org/10.1021/acs.jctc.6c00505
J. Chem. Theory Comput. XXXX, XXX, XXX−XXX

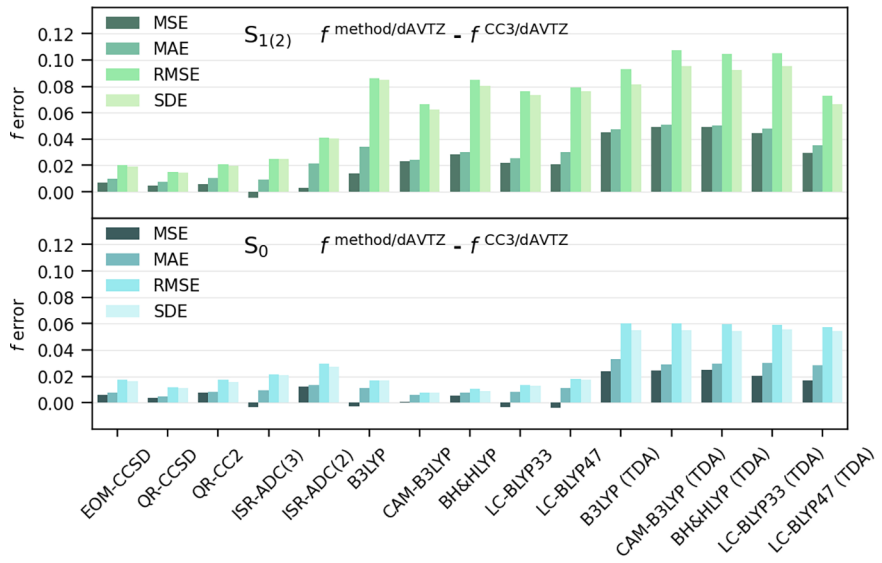

Figure 10. Comparison of MSE, MAE, RMSE, and SDE for f in length gauge for all methods and a subset of transitions. Top: errors obtained on $S_{1/2}$ geometries. Bottom: errors obtained on S_0 structures with the same subset of transitions. All values are compared with a QR-CC3/dAVTZ reference. For full results, see the Supporting Information.

https://doi.org/10.1021/acs.jctc.6c00505
J. Chem. Theory Comput. XXXX, XXX, XXX−XXX